ISSN 1392 - 1207. MECHANIKA. 2006. Nr.2(58)

Insertion investigation of cylindrical parts to be assembled with clearance

B. Bakšys*, S. Kilikevičius**
**Kaunas University of Technology, Kęstučio 27, 44025 Kaunas, Lithuania, E-mail: bronius.baksys@ktu.lt*
***Kaunas University of Technology, Kęstučio 27, 44025 Kaunas, Lithuania, E-mail: sigitas.kilikevicius@stud.ktu.lt*

1. Introduction

The main stages of automated assembly are matching of connective surfaces and insertion of parts.

Works published about parts insertion process are rare, besides, in the majority of these works, quasi-static assembly is analyzed, where the insertion speed is very low and the influence of inertia and gravity is negligible. Recently, using quasi-static insertion theory, it is attempted to analyse microparts insertion [1], more complex cases of wedging [2]. The vibratory method and the diagram of assembling equipment, which aid to assemble parts avoiding jams, are proposed [3].

However, quasi-static insertion occurs rarely in practice. Successful and competitive manufacture requires to increase productivity and to reduce equipment cost. Most effective solution to increase the productivity of assembly operations is to increase the insertion speed. Insertion of parts is a complex dynamic process, which is under the influence of many factors – gravity, inertia, insertion speed, stiffness of basing device, friction, etc. Parts can get wedged if improper parameters influencing insertion process are selected. Therefore, the parts and assembly equipment can be damaged. To develop low-priced, effective and reliable assembly equipment, it is necessary to investigate and in depth understand parts insertion mechanism.

Paper [4] investigates dynamics of insertion process. Differential equations of peg's movement in a hole are presented, while the peg contacts with the hole in one and two points in all possible arrangements of connecting surfaces. Geometric compatibility conditions for the successful insertion were presented. However, this paper does not investigate chamfer crossing stage, does not determine the influence of different parameters on the insertion process.

The model of dynamic insertion is investigated more properly in papers [5, 6]. However a few simulation results are presented in these articles, besides the simulation results are different. Paper [5] investigates dynamic model of insertion process. Diagrams of variation in time of insertion force along axial direction and tilt angle of the peg, in chamfer crossing, one point and two point contact stages are given. A device for high speed chamferless assembly is proposed. Paper [6] investigates the insertion process in greater detail. Diagrams of variation in time of insertion forces, tilt angle of peg, lateral deviation along the horizontal direction and depth of insertion are given. It is noticed that the motion of mobile based peg during two point contact stage is uneven. The influence of different parameters on tilt angle of the peg and insertion forces was determined, but diagrams of their dependences were not given. Dependences of insertion time on basing device characteristics, insertion speed and others parameters were not determined.

This paper investigates the influence of different parameters on insertion duration and reliability of the insertion process of cylindrical parts with clearance.

2. Mathematical model of insertion process

Insertion of mobile based peg, which is moved in constant velocity v, into immobile bush is investigating (Fig. 1). The peg is hold by the gripper and only can turn around the centre of compliance C.

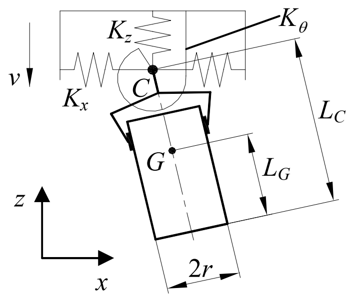

Fig. 1 Mobile based peg

Elastic components of the insertion force along x axis F_x, along z axis F_z and torsion moment M about point C, can be written

$$F_x = K_x(x_C - x_{C0}) \tag{1}$$
$$F_z = K_z(vt + z_C - z_{C0}) \tag{2}$$
$$M = K_\theta(\theta - \theta_0) \tag{3}$$

where, x_C and z_C are the coordinates of point C; x_{C0} and z_{C0} are the coordinates of point C at the initial instant of time; θ is tilt angle of the peg; θ_0 is tilt angle of the peg at the initial instant of time; K_x, K_z, K_θ are lateral stiffness, axial stiffness and angular stiffness respectively.

In case of peg contact with the chamfer (Fig. 2, a), coordinates of the centre of compliance C and the centre of mass G are expressed by the dependences

$$x_C = R + \varepsilon - L_C \sin\theta \tag{4}$$
$$z_C = L_C \cos\theta + r\sin\theta + z_A \tag{5}$$
$$x_G = R + \varepsilon - L_G \sin\theta \tag{6}$$
$$z_G = L_G \cos\theta + r\sin\theta + z_A \tag{7}$$

where L_C is the distance from the lower end surface of the peg to the centre of compliance; L_G is the distance from the lower end surface of the peg to the centre of mass; R and r are the radius of the hole and the peg respectively; ε is the displacement from the centre of the lover end of the peg to the centre line of the hole, along x axis direction.

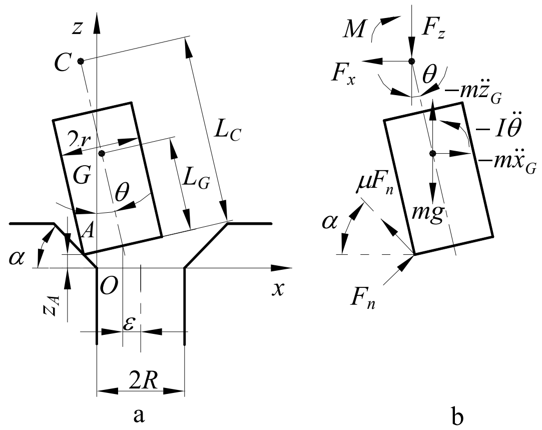

Fig. 2 Peg contact with chamfer

Vertical coordinate of point A, where the peg contacts with the chamfer

$$z_A = (r\cos\theta - \varepsilon - R)\tan\alpha \tag{8}$$

where α is the chamfer angle.

Initial coordinates of the centre of compliance

$$x_{C0} = R + \varepsilon_0 - L_C \sin\theta_0 \tag{9}$$

$$\begin{aligned} z_{C0} &= L_C\cos\theta_0 + r\sin\theta_0 + \\ &+ (r\cos\theta_0 - \varepsilon_0 - R)\tan\alpha \end{aligned} \tag{10}$$

where ε_0 is the initial value of ε.

During chamfer crossing stage (Fig. 2, b), the peg is influenced by elastic components of insertion force and torque (F_x, F_z, M), gravity mg, inertia forces $m\ddot{x}_G$, $m\ddot{z}_G$, inertia torque $I\ddot{\theta}$, reaction force F_n, friction force μF_n; where m is the mass of the peg and gripper, I is inertia moment of the peg and gripper about the centre of mass, g is gravitational constant, μ is dry friction constant.

Applying D'Alembert principle, the peg contact with the chamfer is determined by the following equations

$$\left.\begin{aligned} &K_1F_n - F_x - m\ddot{x}_G = 0 \\ &K_2F_n - F_z - m\ddot{z}_G - mg = 0 \\ &(F_x\cos\theta + F_z\sin\theta)(L_C - L_G) + K_3F_n - \\ &- M - I\ddot{\theta} = 0 \end{aligned}\right\} \tag{11}$$

where $K_1 = \sin\alpha - \mu\cos\alpha$; $K_2 = \cos\alpha + \mu\sin\alpha$; $K_3 = (L_GK_1 - rK_2)\cos\theta + (L_GK_2 + rK_1)\sin\theta$.

Initial conditions: $\theta(0) = \theta_0$, $\dot{\theta}(0) = \dot{\theta}_0$, $\varepsilon(0) = \varepsilon_0$, $\dot{\varepsilon}(0) = \dot{\varepsilon}_0$.

When $z_A = 0$, the process steps into one point contact stage.

In case of one point contact (Fig. 3, a), geometric constraints

$$\varepsilon = r\cos\theta + h\sin\theta - R \tag{12}$$

$$B = 2R - h\sin\theta - 2r\cos\theta \tag{13}$$

where h is insertion depth, which is the distance from the point of contact to the lower end of the peg along axial direction of the peg.

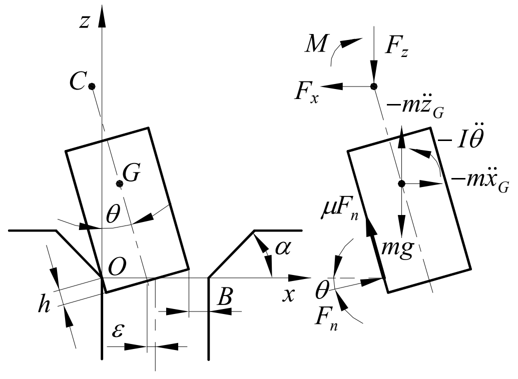

Fig. 3 One point contact stage

The coordinates of points C and G

$$x_C = r\cos\theta - (L_C - h)\sin\theta \tag{14}$$

$$z_C = (L_C - h)\cos\theta + r\sin\theta \tag{15}$$

$$x_G = r\cos\theta - (L_G - h)\sin\theta \tag{16}$$

$$z_G = (L_G - h)\cos\theta + r\sin\theta \tag{17}$$

After the evaluation of acting forces in one point contact stage (Fig. 3, b), movement of the peg in the hole is determined by the following equations

$$\left.\begin{aligned} &K_4F_n - F_x - m\ddot{x}_G = 0 \\ &K_5F_n - F_z - m\ddot{z}_G - mg = 0 \\ &(F_x\cos\theta + F_z\sin\theta)(L_C - L_G) + \\ &+ (L_G - h - \mu r)F_n - M - I\ddot{\theta} = 0 \end{aligned}\right\} \tag{18}$$

where $K_4 = \cos\theta - \mu\sin\theta$; $K_5 = \sin\theta + \mu\cos\theta$.

The initial conditions become: $\theta = \theta_-$, $\dot{\theta} = 0$, $h = 0$, $\dot{h} = (\dot{\varepsilon}_- + r\dot{\theta}_-\sin\theta_-)/\cos\alpha$; where subscript "–" represents values of variables defined just before the one point contact stage.

When B=0 (Fig. 3, a), the process steps into two point contact stage.

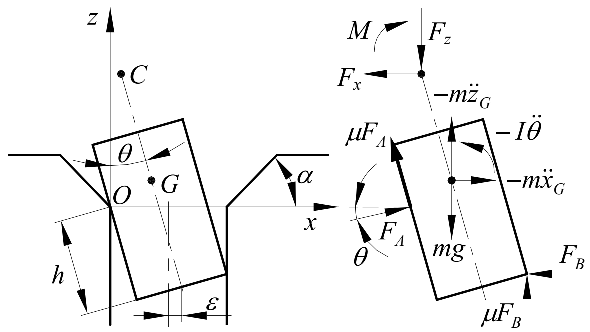

Fig. 4 Two point contact stage

In case of two point contact (Fig. 4, a), the coordinates of points C and G

$$x_C = 2R - r\cos\theta - L_C \sin\theta \tag{19}$$
$$z_C = (L_C - h)\cos\theta + r\sin\theta \tag{20}$$
$$x_G = 2R - r\cos\theta - L_G \sin\theta \tag{21}$$
$$z_G = (L_G - h)\cos\theta + r\sin\theta \tag{22}$$

Geometrical relations in two point contact stage

$$h = 2(R - r\cos\theta)/\sin\theta \tag{23}$$
$$\varepsilon = R - r\cos\theta \tag{24}$$

After the evaluation of acting forces in two point contact stage (Fig. 4, b), movement of the peg in the hole is determined by the following equations

$$\left.\begin{aligned} &K_4F_A - F_B - F_x - m\ddot{x}_G = 0\\ &K_5F_A + \mu F_B - F_z - m\ddot{z}_G - mg = 0\\ &(F_x\cos\theta + F_z\sin\theta)(L_C - L_G) - M - I\ddot{\theta} +\\ &+(L_G - h - \mu r)F_A - (L_GK_4 - rK_5)F_B = 0 \end{aligned}\right\} \tag{25}$$

The initial conditions: $\theta = \theta_-$; $\dot{\theta} = \left[\dot{\theta}_-(h_- \sin\theta_- + 2r\cos\theta_-) - \dot{h}_- \cos\theta_-\right]\cdot(\sin\theta_- / h_-)$; where subscript "–" represents values of variables defined just before the two point contact stage.

The transition from the two point contact stage to the one point contact stage is possible, if F_B=0. Insertion process terminates when the specified depth of insertion h_i is reached.

3. Simulation of insertion process

Programs for the simulation of insertion process were written using MatLab software. A number of numerical experiments, while the peg was crossing the chamfer, the peg was in one point contact and two points contact with the bush hole, was performed. The influence of different factors on insertion process was investigated, for purpose to determine when the time of insertion process is the shortest and to determine conditions for the most reliable insertion, avoiding wedging. All experiments were done using the same initial values of parameters of insertion process by changing only the analysing parameter. The following initial values of the parameters of insertion process were used: $m = 0.1$ kg; $r = 0.0099$ m; $R = 0.01$ m; $I = 0.002$ kg·m^2; $L_G = 0.05$ m; $L_C = 0.025$ m; $\alpha = \pi/4$ rad; $\mu = 0.1$; $v = 0.3$ m/s; $\theta_0 = 0.01$ rad; $\dot{\theta}_0 = 0.01$ m/s; $\varepsilon_0 = -0.001$ m; $\dot{\varepsilon}_0 = 0.001$ m/s; $K_x = 2000$ N/m; $K_z = 2000$ N/m; $K_\theta = 20$ N·m/rad; $h_i = 0.05$ m.

The process of insertion starts when the peg touches the chamfer. The peg slides down the chamfer until the cylindrical surface of peg touches the hole. Insertion process steps into the one point contact stage, and time instant t_1 is defined. Parameter t_1 is the chamfer crossing duration.

An increase of the peg and gripper mass m yields an increase of the chamfer crossing duration (Fig. 5). Chamfer crossing duration t_1 increases when lateral stiffness K_x is increasing (Fig. 6, a). Chamfer crossing duration t_1 increases when the coefficient of friction μ is increasing. Chamfer crossing duration t_1 increases when initial lateral misalignment ε_0 increases due to the increase of the distance whereby the peg slides.

Chamfer crosses faster when the axial stiffness K_z is increasing (Fig. 6, b).

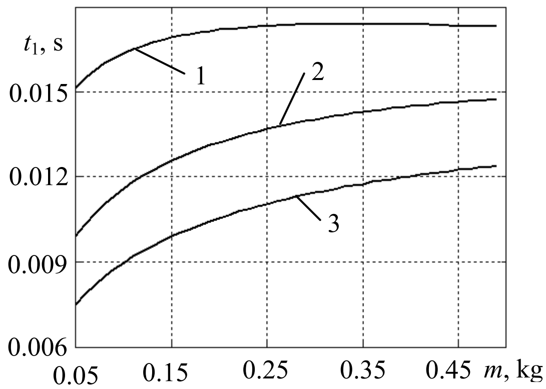

Fig. 5 Dependences of chamfer crossing duration t_1 on the mass of the peg and gripper m, under different axial stiffness K_z values: *1* – K_z = 500 N/m; *2* – K_z = = 2000 N/m; *3* – K_z = 5000 N/m

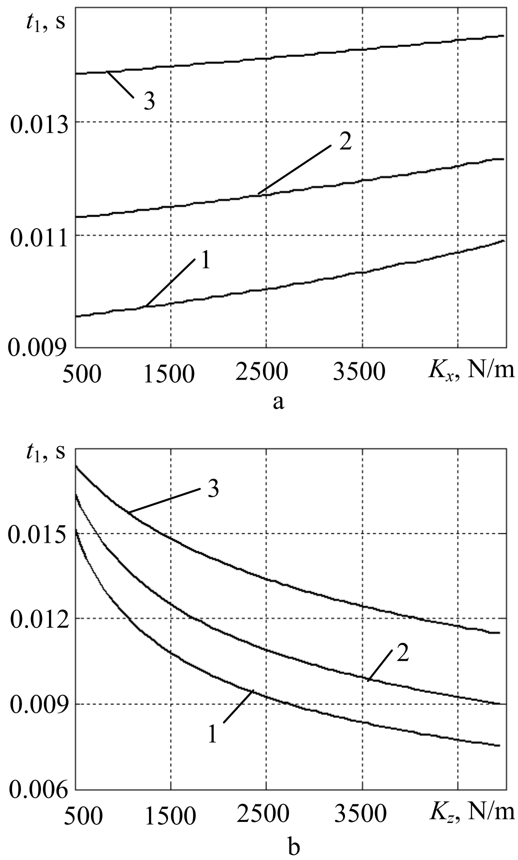

Fig. 6 Dependences of chamfer crossing duration t_1: a – on lateral stiffness K_x; b – on axial stiffness K_z, under different values of m: *1* – m = 0.05 kg; *2* – m = 0.1 kg; *3* – m = 0.3 kg

Peg contacts with the hole in one point until the lower edge of the peg reaches internal surface of the hole. Insertion process steps into the two point contact stage, and time instant t_2 is defined. Duration t_2 consists of chamfer crossing duration t_1 and the duration of two point contact stage. Parameter t_2 is the duration from the beginning of insertion process to the beginning of two point contact stage. Duration t_2 is mostly influenced by the depth, wherein the two point contact appears. This is well represented by dependences of duration t_2 on assembly clearance δ, under different lateral stiffness K_x values (Fig. 7).

Parts are completely assembled when the required depth of insertion h_i is reached. Insertion process duration t_3 is the duration from the beginning of chamfer crossing stage to the termination of insertion process. It consists of the duration of two point contact stage and the duration t_2.

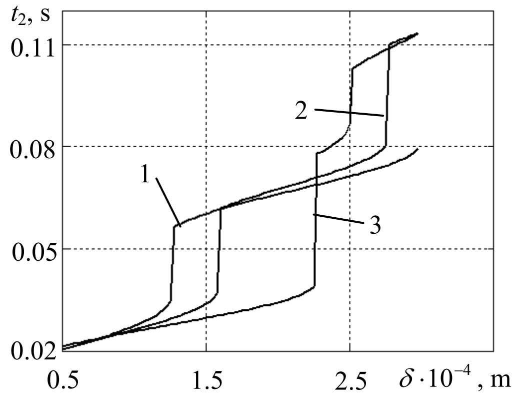

Fig. 7 Dependences of duration of time t_2 on clearance δ, under different lateral stiffness K_x values: *1* – K_x = = 500 N/m; *2* – K_x = 2000 N/m; *3* – K_x = 5000 N/m

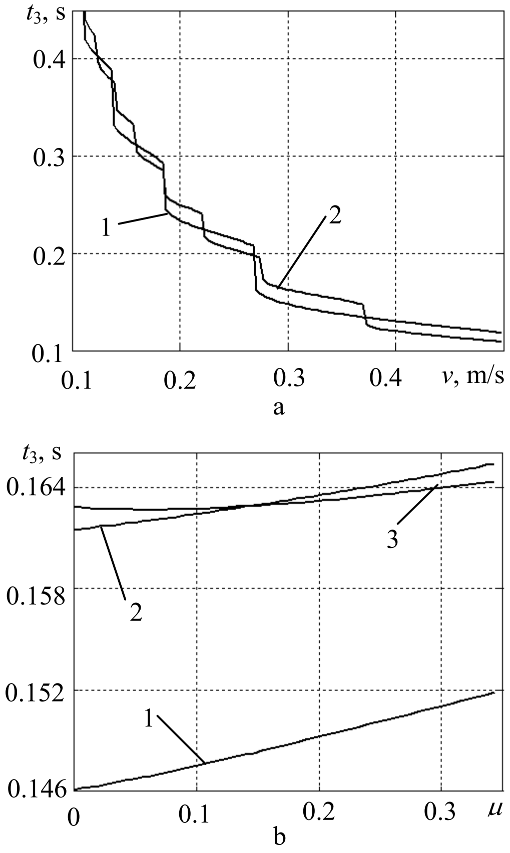

Fig. 8 Dependences of insertion process duration t_3: a – on insertion speed v; b – on coefficient of friction μ, under different axial stiffness K_z values: *1* – K_z = =500 N/m; *2* – K_z = 2000 N/m; *3* – K_z = 5000 N/m

Most effective way to shorten insertion process duration t_3, and to increase the productivity of assembly operations, is to increase the insertion speed. When insertion speed is increasing, the insertion process duration distinctly shortens (Fig. 8, a). Jumps of insertion process duration t_3, visible in diagram, occur due to uneven movement of the peg in the hole. Friction between the parts also makes influence on duration of the insertion process. The insertion process takes more time when the coefficient of friction is increasing (Fig. 8, b) Duration of the insertion process is the most reasonable when the distance from the lower end surface of the peg to the centre of compliance L_C is close to 0 (Fig. 9).

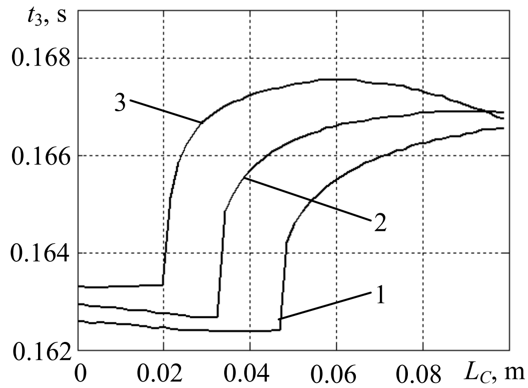

Fig. 9 Dependences of insertion process duration t_3 on L_C, under different lateral stiffness K_x values: *1* – K_x = =2000 N/m; *2* – K_x = 3000 N/m; *3* – K_x = 5000 N/m

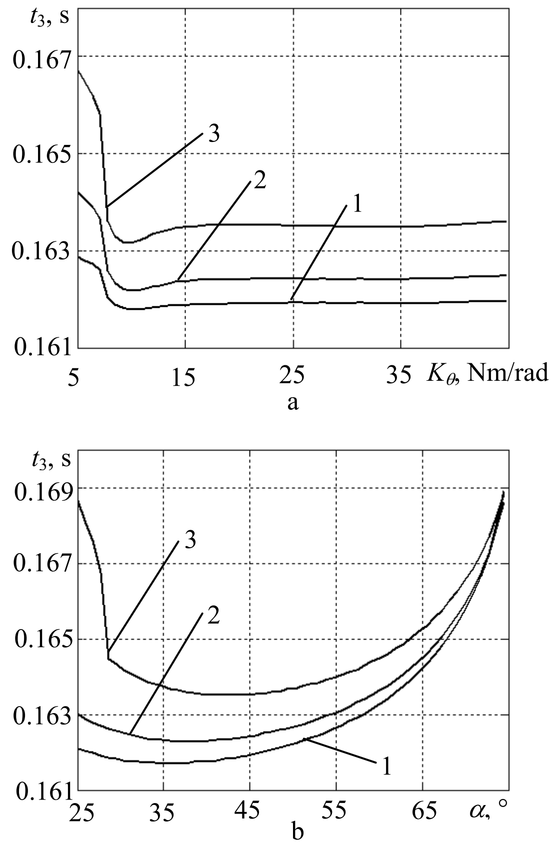

Fig. 10 Dependences of insertion process duration t_3: a – on angular stiffness; b – on angle of chamfer α, under different coefficient of friction μ values: *1* – μ = 0.05; *2* – μ = 0.1; *3* – μ = 0.2

Adjustment of angular stiffness K_θ can shorten duration of the insertion process. Generally, the insertion process takes a little bit more time if angular stiffness K_θ is very low (Fig. 10, a). If the value of angular stiffness K_θ is very high, duration of the insertion process significantly increases, because it takes more time to compensate angular errors of the peg. Usually, when chamfer angle is approximately in the range of 40-50°, insertion process duration is the shortest (Fig. 10, b). This occurs due to the increase of chamfer crossing duration t_1 under high or low values of chamfer angle. Chamfer crossing duration increases under low values of chamfer angle, because it is more difficult to cross the less sloping surface of the chamfer. When the chamfer angle is high, the peg must to slide longer distance under the same value of initial lateral misalignment ε_0.

It is more difficult to determine the influence of such insertion process parameters as lateral K_x, axial K_z stiffness, mass m, clearance δ, initial deviations ε_0, θ_0 on insertion process duration, because it varies with jumps under the influence of these parameters (Fig. 11).

Distance to the centre of mass L_G and moment of inertia I do not have high influence on duration of insertion process.

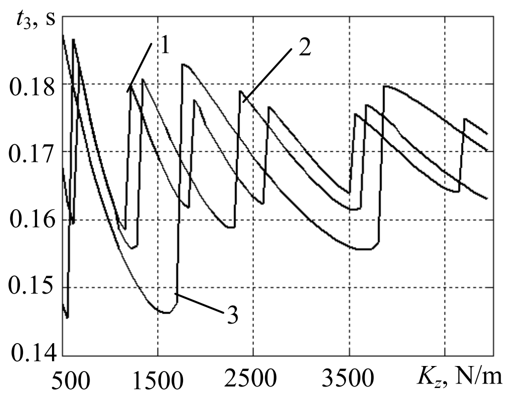

Fig. 11 Dependences of insertion process duration t_3 on axial stiffness K_z, under different values of m: *1* – m = 0.05 kg; *2* – m = 0.1 kg; *3* – m = 0.3 kg

Insertion process can fail due to wedging. Wedging usually occurs in the two point contact stage. Wedging occurs when reaction forces are inside the friction cones and act in the same line. Therefore the peg can not move. This occurs when tilt angle of the peg exceeds critical angle: $\theta > \theta_w \approx (R - r)/(r\mu)$.

Insertion process will fail also, if the peg will jump out of the hole due to its oscillating movement along z axis direction. Consequently, it is necessary that maximum value of tilt angle θ_{max} would not exceed the critical limit.

Regard to that, it is possible to come to a conclusion that lower θ_{max} values yield higher probability of successful insertion. It is possible to decrease the value of θ_{max} by applying suitable parameters of insertion process.

When angular stiffness K_θ of the system is increasing, maximum value of tilt angle of the peg decreases (Fig. 12, a). Maximum value of tilt angle of the peg θ_{max} increases, when lateral stiffness K_x is increasing (Fig. 12, b). The value of θ_{max} increases, because the peg is forced to turn around the centre of compliance by larger angle to accomplish the insertion process, during two point contact stage, under higher lateral stiffness. Besides, under the increase of lateral stiffness, oscillation amplitude of the peg movement in z axis direction significantly increases. Therefore, the probability of peg coming out of the hole increases.

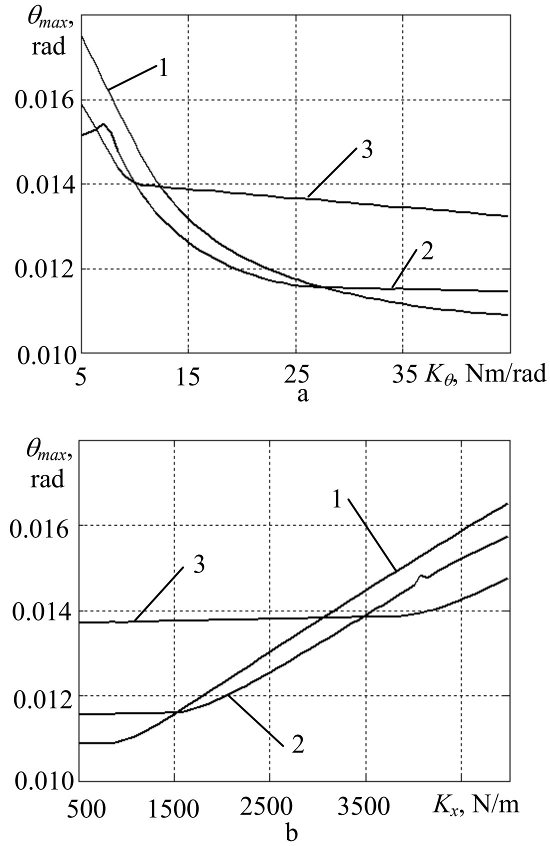

Fig. 12 Dependences of maximum tilt angle of the peg θ_{max}: a – on angular stiffness K_θ; b – on lateral stiffness K_x, under different values of m: *1* – m = = 0.05 kg; *2* – m = 0.1 kg; *3* – m = 0.3 kg

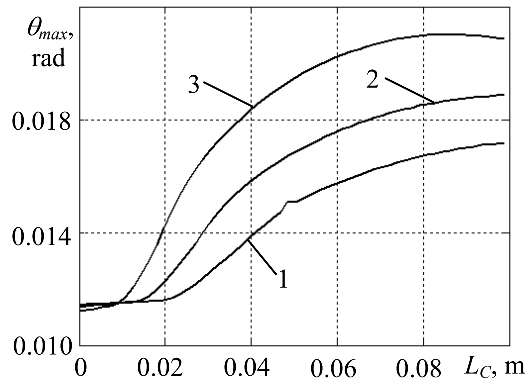

Fig. 13 Dependences of maximum tilt angle of the peg θ_{max} on L_C, under different lateral stiffness K_x values: *1* – K_x = 2000 N/m; *2* – K_x = 3000 N/m; *3* – K_x = = 5000 N/m

Distance from the lower end surface to the centre of compliance L_C makes significant influence on the value of tilt angle of the peg. When L_C is close to 0, the value of θ_{max} reaches the minimal value (Fig. 13). When total mass of the peg and gripper m is increasing, θ_{max} increases (Fig. 14, a). At the beginning, an increase of inertia moment I about mass centre, yields significant decrease of θ_{max}, later the value of θ_{max} does not change much

(Fig. 14, b). The value of θ_{max} also increases under higher values of initial deviations ε_0, θ_0. When the clearance ratio becomes higher, the value of θ_{max} increases more significant only under higher values of lateral stiffness K_x. Axial stiffness K_z, insertion speed v, distance to the centre of mass L_G do not have high influence on the value of θ_{max}.

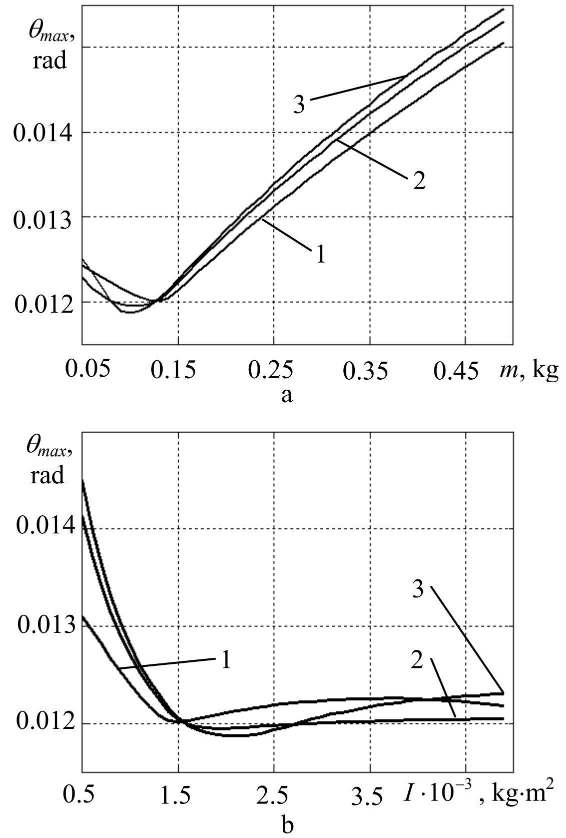

Fig. 14 Dependences of maximum tilt angle of the peg θ_{max}: a – on total mass of the peg and gripper m; b – on inertia moment I, under different axial stiffness K_z values: *1* – K_z = 500 N/m; *2* – K_z = =2000 N/m; *3* – K_z = 5000 N/m

Reliability of insertion depends on the depth h_2, when the two point contact appears. It is noticed, that wedging usually appears when the two point contact appears in small depth. Besides, the probability increases that the peg will jump out of the hole when the two point contact appears in a small depth. Therefore, it is necessary to select such values of insertion process parameters, which influence the higher value of depth h_2.

A high influence on depth h_2 has clearance ratio δ. When the clearance ratio is increasing, two point contact stage appears in higher depth (Fig. 15, a). The depth, when the two point contact appears, decreases when distance L_C is increasing (Fig. 15, b). When lateral stiffness K_x is increasing, two points contact appears in smaller depth (Fig. 16). This appears, because the peg is forced to turn around the centre of compliance by larger angle during the chamfer crossing and the one point contact stage due to the increase of stiffness along lateral direction. Jumps of h_2 appear due to uneven movement of mobile based peg. Two point contact stage appears in smaller depth under small values of angular stiffness due to easier turning of the peg around the centre of compliance (Fig. 17). Naturally, depth h_2 significantly decreases when initial tilt angle θ_0 is increasing. Other parameters of insertion process do not have high influence on depth h_2.

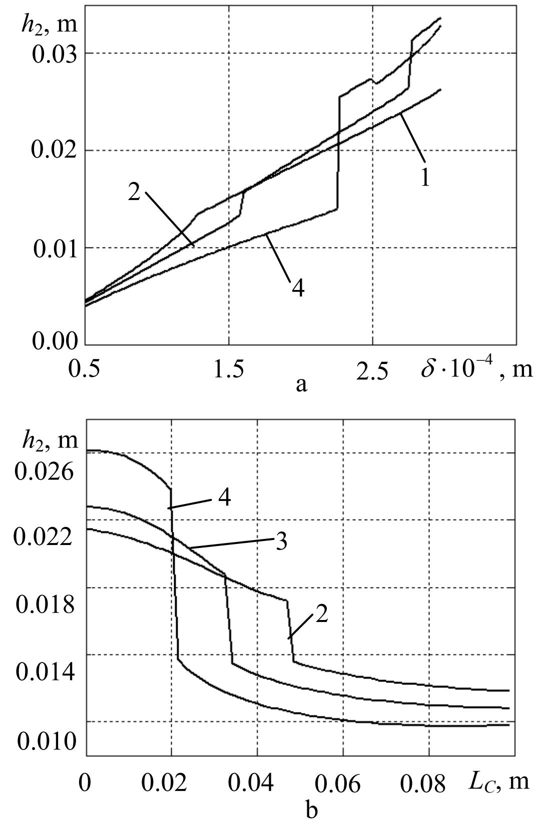

Fig. 15 Dependences of depth h_2: a – on δ; b – on L_C, under different values of K_x: *1* – K_x = 500 N/m; *2* – K_x = =2000 N/m; *3* – K_x = 3000 N/m; *4* – K_x = 5000 N/m

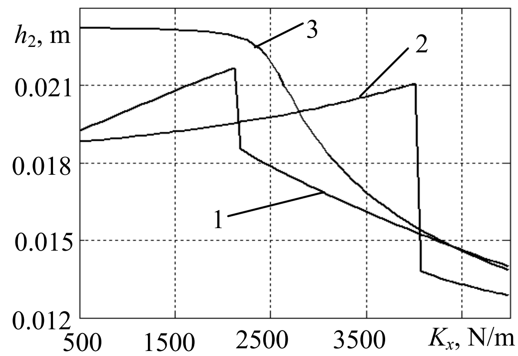

Fig. 16 Dependences of depth h_2, on lateral stiffness K_x, under different values of m: *1* – m = 0.05 kg; *2* – m = 0.1 kg; 3 – m = 0.3 kg

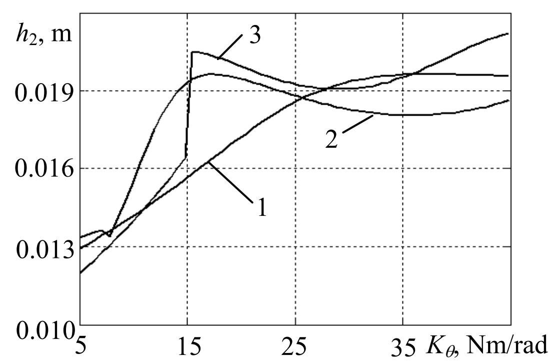

Fig. 17 Dependences of depth h_2, on angular stiffness K_θ, under different values of K_z: *1* – K_z = 500 N/m; *2* – K_z = 2000 N/m; *3* – K_z = 5000 N/m

4. Conclusions

1. Mathematical model of cylindrical parts insertion was formed, programs for simulation of the insertion process were written using MatLab software. Numerical experiments of insertion of cylindrical parts with clearance were implemented. Conditions for the most reliable insertion process and for the shortest duration of insertion process were determined.

2. To achieve the shortest duration of insertion process it is necessary to increase insertion speed v, to adjust rational angular stiffness K_θ, to select L_C close to 0 and to decrease friction.

3. It was determined that the probability of wedging and the probability of peg jumping out of the hole during insertion process, decrease when the maximum value of tilt angle of the peg θ_{max} is smaller, i.e. when angular stiffness K_θ increases, lateral stiffness K_x decreases, distance from the lower end surface of the peg to the centre of compliance L_C is close to 0, mass of the peg and gripper m decreases, inertia moment I increases.

4. It was determined that the probability of wedging and the probability of peg jumping out of the hole increase when the two point contact appears in small depth. Two point contact stage appears in higher depth when clearance ratio δ increases, L_C is close to 0, lateral stiffness K_x decreases, angular stiffness K_θ increases and initial tilt angle θ_0 decreases.

References

1. **Lee, W.H., Kang, B.H., Oh, Y.S., Stephanou, H., Sanderson, A.C., Skidmore, G., Ellis, M.** Micropeg manipulation with a compliant microgripper.-Proc. of the 2003 IEEE Int. Conf. on Robotics and Automation. -Taipei, 2003. p.3213-3218.
2. **Fei, Y., Zhao, X.** Jamming analyses for dual peg-in-hole insertions in three dimensions. -Robotica. -Cambridge University Press, 2005, v.23. p.81-93.
3. **Bakšys, B., Fedaravičius, A., Povilionis, A.B.** Connection conditions of mobile based parts.-Mechanika.-Kaunas: Technologija, 2002, No5(37). p.19-25.
4. **Shahinpoor, M., Zohoor, H.** Analysis of dynamic insertion type assembly for manufacturing automation. -Proc. of the 1991 IEEE Int. Conf. on Robotics and Automation. -Sacramento, 1991, p.2458-2464.
5. **Trong, D.N., Betemps, M. Jutard, A.** Analysis of dynamic assembly using passive compliance.-Proc. of the 1995 IEEE Int. Conf. on Robotics and Automation. -Nayoga, 1995, p.1997-2002.
6. **Du, K.L., Zhang, B.B., Huang, X., Hu, J.** Dynamic analysis of assembly process with passive compliance for robot manipulators.-Proc. 2003 IEEE Int. Symposium on Computational Intelligence in Robotics and Automation.-Kobe, 2003, p.1168-1173.

B. Bakšys, S. Kilikevičius

SU TARPELIU RENKAMŲ CILINDRINIŲ DETALIŲ SUJUNGIMO TYRIMAS

R e z i u m ė

Straipsnyje nagrinėjamas automatiškai renkamų cilindrinių detalių su tarpeliu sujungimas, kai įvorė bazuojama nejudamai, o strypas paslankiai. Sudarytas sujungimo proceso matematinis modelis, aprašantis strypo kontaktą su įvorės nuožula, strypo vieno ir dviejų taškų kontaktą su įvorės skyle. Atlikti skaitmeniniai su tarpeliu renkamų cilindrinių detalių sujungimo eksperimentai. Nustatyta kokiomis sąlygomis sujungimo procesas trunka trumpiausiai ir yra patikimiausias.

B. Bakšys, S. Kilikevičius

INSERTION INVESTIGATION OF CYLINDRICAL PARTS TO BE ASSEMBLED WITH CLEARANCE

S u m m a r y

Insertion of cylindrical parts to be automatically assembled with clearance, while bush is based immobile and the peg is based mobile, is analysed in the paper. Mathematical model of cylindrical parts insertion, which determines peg contact with the chamfer of the bush, peg one point and two point contact with the bush hole, was formed. Numerical experiments of insertion of cylindrical parts to be assembled with clearance were implemented. Conditions for the shortest duration of insertion process and for the most reliable insertion process were determined.

Б. Бакшис, С. Киликевичюс

ИССЛЕДОВАНИЕ СОЕДИНЕНИЯ С ЗАЗОРОМ СОБИРАЕМЫХ ЦИЛИНДРИЧЕСКИХ ДЕТАЛЕЙ

Р е з ю м е

В статье рссматривается процесс соединения автоматически собираемых цилиндрических деталей с зазором при неподвижно базируемой втулке и податливом стержне. Составлена математическая модель процесса соединения, описываюшая контакт стержня с фаской втулки, одноточечный и двухточечный контакт стержня с отверствием втулки. Проведены численные эксперименты при соединении цилиндрических деталей с зазором. Определены условия, при которых обеспечивается наибольшая надежность и наименьшая продолжительность процесса соединения.

Received November 17, 2005